

Preparation and Characterization of Gallium Magnesium Zinc Oxide Transparent Conductive Thin Films

Gu Jinhua¹, Zhu Ya², Lu Zhou², Kang Huai²

(1 Experimental Teaching and Laboratory Management Center, South-Central University for Nationalities, Wuhan 430074, China;
2 College of Electronic Information Engineering, South-Central University for Nationalities, Wuhan 430074, China)

Abstract Gallium magnesium zinc oxide (GaMgZnO) transparent conductive thin films were prepared by magnetron sputtering method. The influence of deposition temperature on the structural and electro-optical properties of the thin films was studied by X-ray diffraction (XRD), four-point probe and ultraviolet-visible spectrometer. The results show that all the thin films are polycrystalline with a hexagonal structure and have a preferred orientation along the *c*-axis perpendicular to the substrate. The deposition temperature significantly affects the crystal quality and electro-optical properties of thin films. When the deposition temperature is at 550 K, the GaMgZnO thin film has the best crystalline quality and electro-optical properties, with the maximum grain size (51.72 nm), the minimum lattice strain (1.11×10^{-3}), the lowest dislocation density ($3.73 \times 10^{14} \text{ line} \cdot \text{m}^{-2}$) and resistivity ($1.63 \times 10^{-3} \Omega \cdot \text{cm}$), and the highest average visible transmittance (82.41%) and figure of merit ($5.06 \times 10^2 \Omega^{-1} \cdot \text{cm}^{-1}$). Furthermore, the optical energy gap of the deposited films were determined and observed to be larger than that of undoped ZnO due to Moss-Burstein effect.

Keywords magnetron sputtering; doped zinc oxide; transparent conductive thin film

中图分类号 TM914 文献标识码 A 文章编号 1672-4321(2018)04-0088-07

镓镁锌氧化物透明导电薄膜的制备及其表征

顾锦华¹, 朱雅², 陆轴², 康淮²

(1 中南民族大学 实验教学与实验室管理中心, 武汉 430074; 2 中南民族大学 电子信息工程学院, 武汉 430074)

摘要 采用磁控溅射方法制备了镓镁锌氧化物(GaMgZnO)透明导电薄膜,通过X射线衍射仪、四探针仪和分光光度计的测试分析,研究了沉积温度对GaMgZnO薄膜微观结构和电光性能的影响。结果显示:所制备的样品均为六角纤锌矿结构的多晶薄膜并具有*c*轴择优取向生长特点,其结晶质量和电光性能与沉积温度密切相关。当沉积温度为550 K时,GaMgZnO薄膜的晶粒尺寸最大(51.72 nm)、晶格应变最小(1.11×10^{-3})、位错密度($3.73 \times 10^{14} \text{ line} \cdot \text{m}^{-2}$)、电阻率最低($1.63 \times 10^{-3} \Omega \cdot \text{cm}$)、可见光区平均透过率(82.41%)、品质因数最大($5.06 \times 10^2 \Omega^{-1} \cdot \text{cm}^{-1}$),具有最好的结晶质量和光电综合性能。另外采用光学表征方法获得了薄膜样品的光学能隙,结果表明由于受Burstein-Moss效应的影响,GaMgZnO薄膜的光学能隙均大于未掺杂ZnO的数值。

关键词 磁控溅射; 掺杂氧化锌; 透明导电薄膜

Zinc oxide (ZnO) is an VI group semiconductor material with wide direct energy gap and wurtzite structure. The high stability, melting point and excitation energy make it a promising ultraviolet and blue optoelectronic material. In addition, ZnO

semiconductor thin films have a wide range of applications in a variety of optoelectronics devices such as flat panel displays^[1,2], solar cells^[3,4], light-emitting diodes^[5,6], thin film transistors^[7] and chemical sensors^[8-10]. A transparent conductive

收稿日期 2017-10-26

作者简介 顾锦华(1972-),女,讲师,研究方向:光电子材料,E-mail: jinhwagu@163.com

基金项目 湖北省自然科学基金资助项目(2011CDB418);中央高校基本科研业务专项资金资助项目(CZP17002)

electrode is a necessary component of solar cells. Usually, it consists of a transparent conducting film (TCF) and a glass substrate. The most important commercial material for TCFs nowadays is indium-tin oxide (ITO), owing to its unique characteristics of high visible transmittance, low resistivity, high infrared reflectance and absorbance in the microwave region^[11,12]. However, ITO is likely to become unavailable because the fast-growing semiconductor industries are faced with the limitation of indium resources and toxicity in the atmosphere^[13,14]. In view of the depletion of ITO, the doped ZnO will be emerging as an alternative transparent electrode. Recently, much attention has been paid to the codoping process in which the two elements are doped into ZnO simultaneously, because the codoped ZnO thin films are expected to show some improvements in electrical and optical performance of TCFs. Up to now, the vanadium-aluminum^[15], aluminum-indium^[16], gallium-indium^[17], aluminum-gallium^[18], boron-gallium^[19], magnesium-aluminum^[20], aluminum-titanium^[21] and gallium-titanium^[22] codoping cases have been reported. As is known, although many experimental studies have been conducted on the synthesis and electrical properties of the codoped ZnO thin films, there are few quantitative studies on their electro-optical properties. In this study, the gallium magnesium zinc oxide (GaMgZnO) transparent conductive thin films were prepared on glass substrates by magnetron sputtering technique. The influence of deposition temperature on the microstructure, electrical and optical properties of the thin films was investigated by X-ray diffraction (XRD), four-probe meter and ultraviolet-visible spectrometer.

1 Experiment

The GaMgZnO samples were deposited on the clean glass substrates by using radio frequency magnetron sputtering technique. A sintered GaMgZnO ceramic sputter target (2 wt% Ga₂O₃: 2 wt% MgO : 96 wt% ZnO, 99.99% purity) was employed as source material. The sputtering chamber was evacuated to a base pressure below 3.1×10^{-4} Pa before argon gas. After vacuum pumping, the sputtering argon gas with a

purity of 99.999% was introduced into the chamber and controlled by the standard mass flow controllers. Before deposition of the GaMgZnO samples, pre-sputtering was conducted for about 10 min to attain stability and to remove impurities. The deposition parameters for preparing GaMgZnO samples were as follows: the substrate-target distance, 75 mm; the sputtering power, 130 W; operating pressure, 3 Pa; and sputtering time, 45 min. In order to investigate the influence of deposition temperature on properties of the GaMgZnO thin films, the deposition temperature was changed from 350 to 650 K. The thickness of the samples was measured by a surface profiler (Alpha-step 500). X-ray diffraction studies were conducted to determine the crystal structure with a D8-Advance diffractometer using Cu K α radiation at 40 kV and 40 mA. The electrical properties were evaluated using a four-point probe measurement system (RH-2035). Optical properties of the films were examined with the normal incident transmittance measured by a double-beam spectrometer (TU-1901). All measurements were performed at room temperature in ambient air.

2 Results and discussion

2.1 Structural properties of the thin films

Fig. 1 shows the XRD patterns of GaMgZnO samples prepared at different deposition temperatures. These XRD peaks are assigned to ZnO according to the Joint Committee of Powder Diffraction Standards Card (JCPDS 36-1451). Note that all the samples exhibit a dominant (002) peak with slight (004) peak in the displayed 2θ region, which indicates that the GaMgZnO thin films have highly preferred orientation with their crystallographic c -axis perpendicular to the substrates, irrespective of deposition temperature. Note also that neither metallic Ga or Mg characteristic peaks nor Ga₂O₃ or MgO peaks was observed from the XRD patterns, which implies that the dopants have not destroyed the ZnO structure and act as typical dopants. Corresponding to the deposition temperatures of 450, 550 and 650 K, the intensity ratio of (004) to (002) ($I_{(004)}/I_{(002)}$) and the intensity of (002) peak ($I_{(002)}$) for the samples are found from Fig. 2 to be 2.14%, 2.59×10^4 cps; 1.96%, 4.63×10^4 cps; and 2.11%,

2.98×10^4 cps, respectively. As is obvious, the values of $I_{(004)} / I_{(002)}$ and $I_{(002)}$ are observed to rise initially and then fall with the increase of deposition temperature. The GaMgZnO sample prepared at 550 K has the minimum $I_{(004)} / I_{(002)}$ and the maximum $I_{(002)}$.

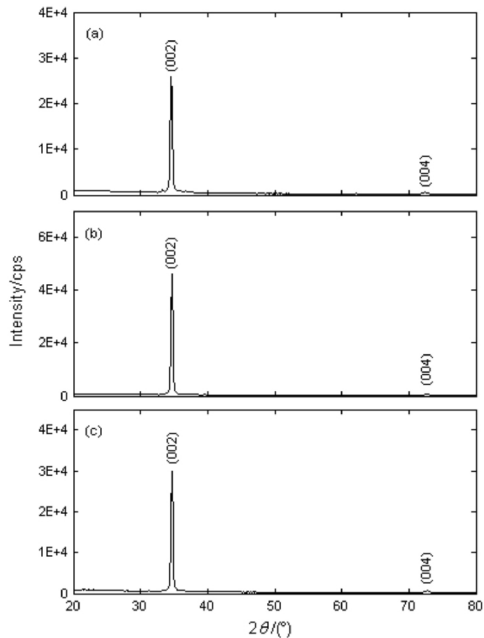


Fig. 1 The XRD patterns of GaMgZnO samples prepared at deposition temperature of (a) 450 K , (b) 550 K and (c) 650 K , respectively

图 1 温度为 (a) 450 K , (b) 550 K 和 (c) 650 K 时 GaMgZnO 样品的 XRD 图谱

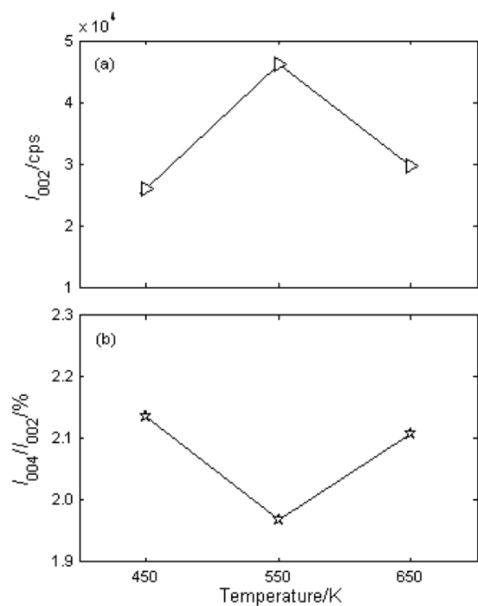


Fig.2 Effect of deposition temperature on $I_{(002)}$ and $I_{(004)} / I_{(002)}$ of GaMgZnO samples

图 2 沉积温度对 GaMgZnO 样品 $I_{(002)}$ 和 $I_{(004)} / I_{(002)}$ 的影响

The grain size of the deposited samples was calculated from the diffraction peaks of (002) plane using the Scherrer's formula^[23, 24]:

$$D = \frac{0.89\lambda}{B \cos\theta} \quad (1)$$

where λ is the wavelength of X-rays used, B is the full-width at half-maximum, and θ is the Bragg's diffraction angle at peak position. The dislocation density (δ) and the lattice strain (ϵ) can be estimated from the following formulae^[25, 26]:

$$\delta = \frac{1}{D^2} \quad (2)$$

$$\epsilon = \frac{\lambda}{D \sin\theta} - \frac{B}{\tan\theta} \quad (3)$$

The values of B , D , δ and ϵ of all the deposited samples are presented in Fig.3 and Fig.4, respectively. With the increment of deposition temperature, the B , δ and ϵ rise in advance and then fall, but the D takes on an opposite trend. When the deposition temperature is 550 K, the deposited GaMgZnO sample exhibits the best crystalline and microstructural properties, with the narrowest B of 2.77×10^{-3} rad, the largest D of 51.72 nm, the minimum δ of 3.73×10^{14} line \cdot m⁻² and the lowest ϵ of 1.11×10^{-3} . The results suggest that the crystal quality of the GaMgZnO thin films is strongly dependent upon the deposition temperature.

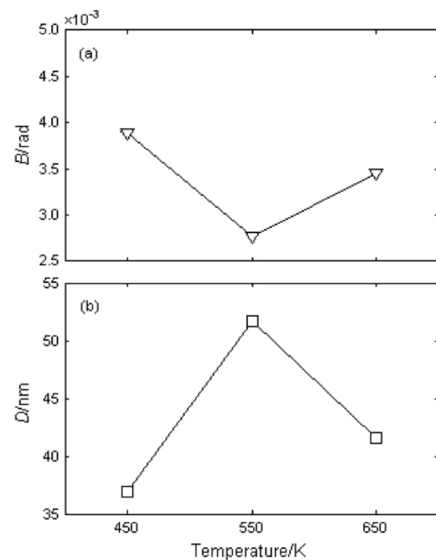


Fig. 3 Effect of deposition temperature on B and D of GaMgZnO samples

图 3 沉积温度对 GaMgZnO 样品 B 和 D 的影响

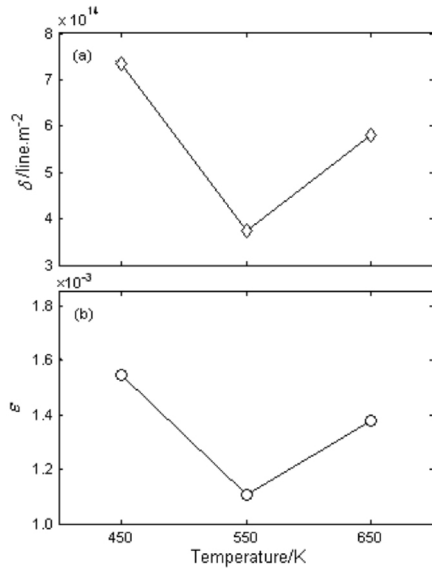


Fig.4 Effect of deposition temperature on δ and ϵ of GaMgZnO samples

图 4 沉积温度对 GaMgZnO 样品 δ 和 ϵ 的影响

2. 2 Electrical and optical properties of the thin films

Fig.5 presents the variation of the resistivity (ρ) with deposition temperature for the GaMgZnO samples. As the deposition temperature from 450 to 550 K, the ρ falls firstly and then rises. The minimum ρ of $1.63 \times 10^{-3} \Omega \cdot \text{cm}$ is obtained at the deposition temperature of 550 K. The decrease of resistivity can be attributed to the improvement of crystalline quality and the increase of carrier concentration.

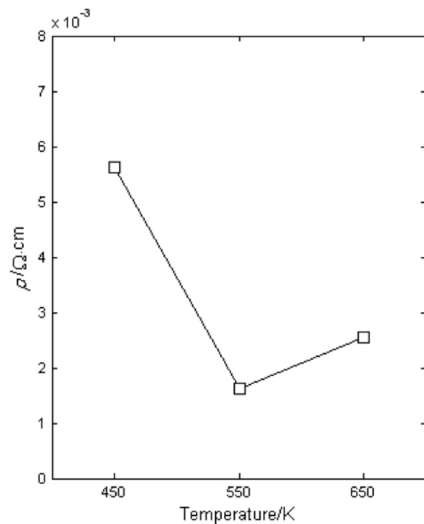


Fig.5 Shows of deposition temperature on ρ of GaMgZnO samples

图 5 沉积温度对 GaMgZnO 样品 ρ 的影响

Fig.6 gives the optical transmittance (T) curves of GaMgZnO samples with glass substrates prepared at

different deposition temperatures. All the transmission spectra show interference pattern with sharp fall of transmittance at the band edge, which is an indication of good crystallinity. Fig.7 (a) shows the variation of the average visible transmittance (T_{av}) with deposition temperature for the GaMgZnO samples. As can be seen, the average transmittance in the visible range (T_{av}) increases slightly with the deposition temperature rising up to 550 K, and then significantly decreases when the deposition temperature is over 550 K. The highest T_{av} of 82.41% for the GaMgZnO thin film with glass substrate can be achieved at the deposition temperature of 550 K. This enhancement in the optical transmittance is closely related to the improvement of crystallinity and the increase of grain size of the deposited films.

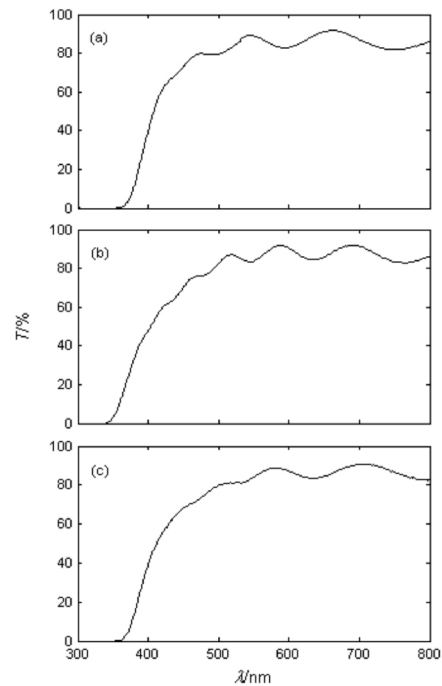


Fig.6 The transmittance curves of GaMgZnO samples prepared at deposition temperature of (a) 450 K, (b) 550 K and (c) 650 K, respectively

图 6 沉积温度为 (a) 450 K, (b) 550 K 和 (c) 650 K 时 GaMgZnO 样品的透过率曲线图

In order to quantify the electro-optical properties of the deposited films, the figure of merit (F_{TC}) is given by the formula^[27 28]:

$$F_{TC} = \frac{T_{av}}{\rho}, \quad (4)$$

where T_{av} is the average visible transmittance and ρ is

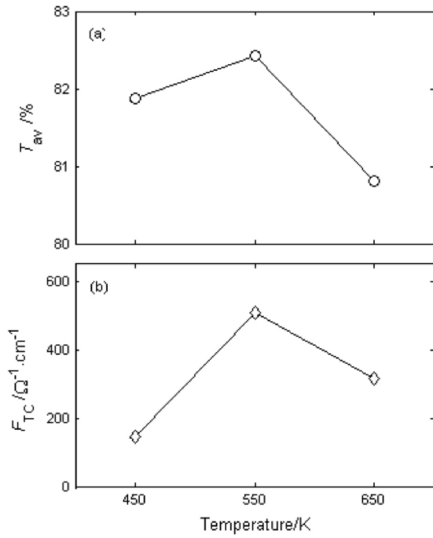


Fig. 7 Effect of deposition temperature on T_{av} and F_{TC} of GaMgZnO samples

图 7 沉积温度对 GaMgZnO 样品 T_{av} 和 F_{TC} 的影响

the resistivity of the films. Fig. 7 (b) displays the variation of F_{TC} with deposition temperature for the deposited samples. As the deposition temperature increases , the F_{TC} first increases and then decreases and reaches its maximum value of $5.06 \times 10^2 \Omega^{-1} \cdot \text{cm}^{-1}$ at the deposition temperature of 550 K. The increase in F_{TC} with deposition temperature was due to increase in T_{av} and decrease in ρ . It is known that the higher the F_{TC} , the better quality of the transparent conductive film. Thus , in this study , it can be concluded that the optimum deposition temperature is 550 K.

2.3 Optical energy gap of the thin films

According to the solid band theory , the direct optical energy gap (E_g) of the deposited films can be determined by the following equations^[29,30]:

$$(\alpha E)^m = B(E - E_g) , \quad (5)$$

$$E = \frac{hc}{\lambda} , \quad (6)$$

where B is a constant , α is the absorption coefficient , E is the photon energy , h is the Planck constant , c is the light velocity , λ is the wavelength of incident light and m is 2 for direct energy gap semiconductors. Fig.8 presents the Tauc plots of $(\alpha E)^2 - E$ for GaMgZnO samples prepared at different deposition temperatures. The linear dependence of $(\alpha E)^2$ on E at higher photon energies indicates that the GaMgZnO thin films are

essentially direct-transition-type semiconductors. The E_g values were obtained by extrapolation method^[31-33] and plotted in Fig. 9. The optical energy gaps of GaMgZnO thin films are found to be ranging from 3.362 to 3.531 eV , larger than that of pure ZnO. The widening of optical energy gap may be attributed to Moss-Burstein effect. This effect is due to the fact that the conduction band filling in highly degenerate semiconductor makes the Fermi level exceed the conduction band minimum. Similar results have been reported in the previously literature^[34-36].

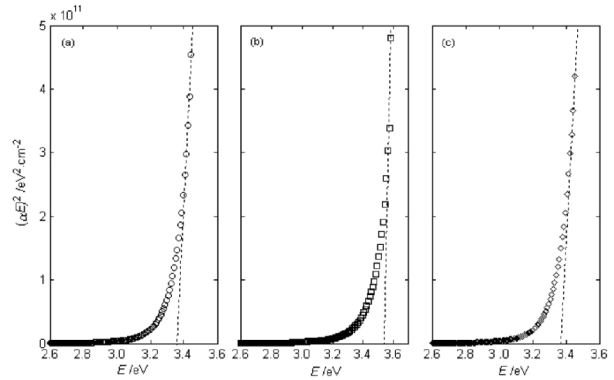


Fig. 8 Tauc plots for GaMgZnO samples prepared at deposition temperature of (a) 450 K , (b) 550 K and (c) 650 K , respectively

图 8 沉积温度为 (a) 450 K , (b) 550 K 和 (c) 650 K 时 GaMgZnO 样品的 Tauc 图

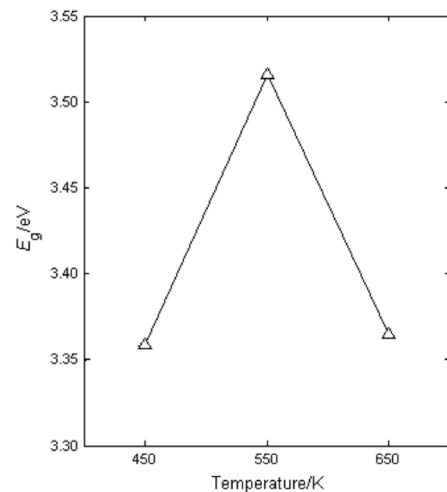


Fig.9 Effect of deposition temperature on E_g of GaMgZnO samples

图 9 沉积温度对 GaMgZnO 样品 E_g 的影响

3 Conclusion

In this work , the transparent conducting

GaMgZnO thin films were prepared by magnetron sputtering technique, and the influence of the deposition temperature on the structural, electrical and optical properties was investigated. It is found that all the deposited films have hexagonal wurtzite structure with highly *c*-axis orientation. The GaMgZnO thin film prepared at the deposition temperature of 550 K possesses the best crystallinity and electro-optical properties, which have the maximum grain size (51.72 nm), the minimum lattice strain (1.11×10^{-3}), the lowest dislocation density ($3.73 \times 10^{14} \text{ line} \cdot \text{m}^{-2}$) and the highest figure of merit ($5.06 \times 10^2 \Omega^{-1} \cdot \text{cm}^{-1}$). The optical energy gaps of the thin films were determined and observed to be larger than that of undoped ZnO due to Moss-Burstein effect. The results demonstrate that the crystal quality, electrical and optical properties of the GaMgZnO thin films are closely related to the deposition temperature.

References

- [1] Yamamoto N, Makino H, Osone S et al. Development of Ga-doped ZnO transparent electrodes for liquid crystal display panels [J]. *Thin Solid Films*, 2012, 520 (12): 4131-4138.
- [2] Chen S, Wei S. The influence of substrate temperature on growth and microstructure of ZnO: Al thin films [J]. *J. South-Cent. Univ. Nationalities (Nat. Sci. Ed.)*, 2015, 34 (3): 72-78.
- [3] Song Y S, Seong N J, Choi K J, et al. Optical and electrical properties of transparent conducting gallium-doped ZnO electrodes prepared by atomic layer deposition for application in organic solar cells [J]. *Thin Solid Films*, 2013, 546 (1): 271-274.
- [4] Zhong Z, Kang H, Lu Z et al. Structure and optical properties of magnesium-doped zinc oxide thin films [J]. *J. South-Cent. Univ. Nationalities (Nat. Sci. Ed.)*, 2017, 36 (1): 64-70.
- [5] Park C Y, Lee J H, Choi B H, Effects of surface treatment of ITO anode layer patterned with shadow mask technology on characteristics of organic light-emitting diodes [J]. *Org. Electron.*, 2013, 14 (12): 3172-3179.
- [6] Long H, Zhang Z, Gu J et al. Effect of graded-composition transition layer on the performance of GaN-based light-emitting diodes [J]. *J. South-Cent. Univ. Nationalities (Nat. Sci. Ed.)*, 2017, 36 (1): 71-75.
- [7] Wu J-L, Lin H-Y, Su B-Y, et al. Comparison of physical and electrical properties of GZO/ZnO buffer layer and GZO as source and drain electrodes of α -IGZO thin-film transistors [J]. *J. Alloy. Compd.*, 2014, 592 (1): 35-41.
- [8] Hjiri M, Mir L E, Leonardi S G, et al. Al-doped ZnO for highly sensitive CO gas sensors [J]. *Sensor. Actuat. B*, 2014, 196 (2): 413-420.
- [9] Hu J, Zhou Y, Liu H, et al. Effect of surface area and gold modification on photocatalytic activity of zinc oxide [J]. *J. South-Cent. Univ. Nationalities (Nat. Sci. Ed.)*, 2010, 29 (2): 6-10.
- [10] Barhoumi A, Leroy G, Duponchel B, et al. Aluminum doped ZnO thin films deposited by direct current sputtering: structural and optical properties [J]. *Superlattice. Microst.*, 2015, 82: 483-498.
- [11] Yang Y, Sun X W, Chen B J, et al. Refractive indices of textured indium tin oxide and zinc oxide thin films [J]. *Thin Solid Films*, 2006, 510 (1-2): 95-101.
- [12] Chen S, Wei S, He X, et al. Effect of modification methods on surface morphology and chemical composition of indium-tin-oxide surfaces [J]. *J. South-Cent. Univ. Nationalities (Nat. Sci. Ed.)*, 2009, 28 (4): 43-46.
- [13] Sahu D R, Huang J L, Development of ZnO-based transparent conductive coatings [J]. *Sol. Energy Mater. Sol. Cells*, 2009, 93 (11): 1923-1927.
- [14] Aghdaee S R, Soleimanian V, Tayebi B. Effect of Al doping on the microstructural, optical and electrical properties of ZnO films [J]. *Superlattice Microst.*, 2012, 51 (1): 149-162.
- [15] Suzuki S, Miyata T, Ishii M, et al. Transparent conducting V-co-doped AZO thin films prepared by magnetron sputtering [J]. *Thin Solid Films*, 2003, 434 (1-2): 14-19.
- [16] Kirbey S D, Van Dover R B. Improved conductivity of ZnO through codoping with In and Al [J]. *Thin Solid Films*, 2009, 517 (6): 1958-1960.
- [17] Suresh A, Wellenius P, Dhawan A, et al. Room temperature pulsed laser deposited indium gallium zinc oxide channel based transparent thin film transistors [J]. *Appl. Phys. Lett.*, 2007, 90 (12): 123512.
- [18] Ebrahimifard R, Golobostanfard M R, Abdizadeh H. Sol-gel derived Al and Ga co-doped ZnO thin films: an optoelectronic study [J]. *Appl. Surf. Sci.*, 2014, 290: 252-259.
- [19] Zhang L, Huang J, Yang J, et al. The effects of thickness on properties of B and Ga co-doped ZnO films grown by magnetron sputtering [J]. *Mater. Sci. Semicond.*

- Process. 2016 42 (Part 3) : 277-282.
- [20] Fang D ,Lin K ,Xue T ,et al. Influence of Al doping on structural and optical properties of Mg-Al co-doped ZnO thin films prepared by sol-gel method [J]. J. Alloy. Compd. 2014 589: 346-352.
- [21] Davoodi A ,Tajally M ,Mirzaee O ,et al. Fabrication and characterization of optical and electrical properties of Al-Ti co-doped ZnO nano-structured thin film [J]. J. Alloy. Compd. 2016 657: 296-301.
- [22] Zhong Z ,Zhang T ,Wang H. Influence of substrate temperature on properties of transparent conducting gallium and titanium doped zinc oxide thin films [J]. J. South-Cent. Univ. Nationalities (Nat. Sci. Ed.) ,2013 , 32 (1) : 58-64.
- [23] Huang T ,Li C ,Wu J ,et al. Controlled synthesis of square palladium nanoplates [J]. J. South-Cent. Univ. Nationalities (Nat. Sci. Ed.) 2013 32 (3) : 5-7.
- [24] Li S ,Yang H ,Wang W ,et al. Effect of argon pressure on properties of flexible ZnO: Al films [J]. Mater. Rev. B , 2014 28 (10) : 6-9.
- [25] Mageshwari K ,Sathyamoorthy R. Physical properties of nanocrystalline CuO thin films prepared by the SILAR method [J]. Mater. Sci. Semicond. Process 2013 ,16: 337-343.
- [26] Gu J ,Lu Z ,Long L ,et al. Preparation and crystalline characteristics of indium-tin-oxide TCO thin films [J]. J. South-Cent. Univ. Nationalities (Nat. Sci. Ed.) , 2016 35(2) : 91-96.
- [27] Mohamed H A. The effect of annealing and ZnO dopant on the optoelectronic properties of ITO thin films [J]. J. Phys. D: Appl. Phys. 2007 40 (14) : 4234-4240.
- [28] Zhong L ,Lan C ,Wang H. Preparation and optical properties of TiO₂-doped zinc oxide semiconductor thin films [J]. J. South-Cent. Univ. Nationalities (Nat. Sci. Ed.) ,2014 33 (1) : 51-57.
- [29] Hua Q ,Fu R ,Yang W ,et al. Effect of sputtering time on the properties of boron-doped ZnO thin films [J]. Mater. Rev. B 2013 27 (9) : 16-22.
- [30] Huang Z ,Liu X ,Wu L ,et al. Preparation and photocatalytic properties of α -Bi₂O₃/TiO₂ nanoparticles [J]. J. South-Cent. Univ. Nationalities (Nat. Sci. Ed.) ,2016 ,35 (1) : 17-21.
- [31] Chen S ,Lan C. Effect of deposition temperature on structure and optical properties of zinc oxide films prepared by sputtering [J]. J. South-Cent. Univ. Nationalities (Nat. Sci. Ed.) 2016 35 (2) : 97-102.
- [32] Tsay C Y ,Wu C W ,Lei C M ,et al. Microstructural and optical properties of Ga-doped ZnO semiconductor thin films prepared by sol-gel process [J]. Thin Solid Films 2010 519 (5) : 1516-1520.
- [33] Sun F ,Hui S. Influence of substrate temperature on performance of transparent conductive ZAO film deposited by RF sputtering [J]. J. South-Cent. Univ. Nationalities (Nat. Sci. Ed.) 2009 28 (2) : 10-13.
- [34] Zhong Z ,Kang H ,Long H. Preparation and properties of magnesium and yttrium doped zinc oxide thin films [J]. J. South-Cent. Univ. Nationalities (Nat. Sci. Ed.) , 2018 37 (1) : 66-72.
- [35] Gu J ,Long L ,Lan C ,et al. Optical properties and microstructure of aluminum-doped zinc oxide thin films [J]. J. South-Cent. Univ. Nationalities (Nat. Sci. Ed.) , 2014 33 (4) : 78-84.
- [36] Aksoy S ,Caglar Y ,Ilican S ,et al. Sol-gel derived Li-Mg co-doped ZnO films: preparation and characterization via XRD ,XPS ,FESEM [J]. J. Alloy. Compd. ,2012 , 512 (1) : 171-178.

(责任编辑 雷建云)